THE UNIVERSITY OF
WARWICK

Original citation:
Shahbaz, T., et al. (2004). The massive neutron star or low-mass black hole in 2S 0921-630. The Astrophysical Journal, 616(2), L123-L126.
Permanent WRAP url:
http://wrap.warwick.ac.uk/50096

Publisher's statement:
http://dx.doi.org/10.1086/426504

A note on versions:
The version presented here is a working paper or pre-print that may be later published elsewhere. If a published version is known of, the above WRAP url will contain details on finding it.

For more information, please contact the WRAP Team at: wrap@warwick.ac.uk

warwick**publications**wrap

highlight your research

http://go.warwick.ac.uk/lib-publications

The massive neutron star or low-mass black hole in 2S 0921–630/V395 Car.

T. Shahbaz[1], J. Casares[1], C. Watson[2], P. A. Charles[3], R. I. Hynes[4], S. C. Shih[3], D. Steeghs[5]

ABSTRACT

We report on optical spectroscopy of the eclipsing Halo LMXB 2S 0921–630/V395 Car, that reveals the absorption line radial velocity curve of the K0III secondary star with a semi-amplitude K_2=92.89± 3.84 km s^{-1} , a systemic velocity γ=34.9±3.3 km s^{-1}and an orbital period $P_{\rm orb}$ of 9.0035±0.0029 day (1-σ). Given the quality of the data we find no evidence for the effects of X-ray irradiation. Using the previously determined rotational broadening of the mass donor, and applying conservative limits on the orbital inclination, we constrain the compact object mass to be 2.0–4.3 M$_\odot$(1-σ), ruling out a canonical neutron star at the 99% level. Since the nature of the compact object is unclear, this mass range implies that the compact object is either a low-mass black hole with a mass slightly higher than the maximum neutron star mass (2.9 M$_\odot$) or a massive neutron star. If the compact object in 2S 0921–630/V395 Car is a black hole, it confirms the prediction of the existence of low-mass black holes, while if the object is a massive neutron star its high mass severely constrains the equation of state of nuclear matter.

Subject headings: accretion: accretion discs – binaries: close stars: individual (2S 0921–630/V395 Car)

[1]Instituto de Astrofísica de Canarias, 38200 La Laguna, Tenerife, Spain. tsh, jcv@iac.es

[2]Department of Physics and Astronomy, University of Sheffield, Sheffield, S3 7RH, England. c.watson@sheffeild.ac.uk

[3]School of Physics and Astronomy, The University of Southampton, Southampton, SO17 1BJ, UK. pac, icshih@soton.ac.uk

[4]McDonald Observatory and Department of Astronomy, The University of Texas at Austin, 1 University Station C1400, Austin, Texas 78712, USA. rih@astro.as.utexas.edu

[5]Harvard-Smithsonian Center for Astrophysics, 60 Garden Street, MS-67, Cambridge, MA 02138, USA. steeghs@cfa.harvard.edu

1. Introduction

A knowledge of the neutron star mass distribution provides a fundamental test of theories of the equation of state of nuclear matter, the applicability of General Relativity as the correct theory of gravity and significant information on the evolutionary history of the progenitor stars. To date, only studies of millisecond radio pulsars have provided accurate mass determinations of neutron stars, reflecting their mass at formation; 1.35 ± 0.04 M$_\odot$ (van Kerkwijk 2001). Although dynamical neutron star masses can also be obtained from accreting X-ray pulsars, there are large uncertainties. In high-mass X-ray binaries (HMXBs) there are uncertainties due to non-Keplerian perturbations in the radial velocity curves caused by effects such as stellar wind contamination and X-ray heating. In low-mass X-ray binaries (LMXBs), the situation is worse because the intense X-ray irradiation usually suppresses the light from the donor (Charles & Coe 2003). It is only in a few exceptional cases where the companion is evolved (and hence more luminous) or during X-ray off-states, when dynamical information can be extracted about the nature of the compact object.

The SAS-3 X-ray source, 2S 0921-630, was identified with a $\sim16^m$ blue star (Li et al. 1978), V395 Car, whose optical spectrum is dominated by HeII 4686Å and Balmer emission (Branduardi-Raymont et al. 1983), characteristics of LMXBs, with occasional superimposed late-type stellar absorption features visible (Thorstensen & Charles 1979). EXOSAT observations showed a broad (>1 day), shallow X-ray eclipse, during which the spectrum softened (Mason et al. 1987), allowing an estimate of the size of the accretion-disc corona (ADC). This was comparable to the eclipsing companion star, thus accounting for the partial X-ray eclipse, and with an inclination of i=70°–90°. Only a handful of ADC sources are known in which the compact object is permanently obscured from our line-of-sight by the accretion disc, and requires the observed X-rays to be scattered in a hot corona (White et al. 1995). By implication, the intrinsic X-ray luminosity is *much* higher.

Limited optical photometry and emission line spectroscopy (Cowley et al. 1982; Branduardi-Raymont et al. 1983) shows that 2S 0921–630/V395 Car has a long orbital period of 9.02 day and deep (~1 mag) dips where the $(B-V)$ colour reddens by up to 0.4 mags, which has been interpreted as the eclipse of the disc by the late-type secondary (Chevalier & Ilovaisky 1982). High-resolution optical spectroscopy revealed the donor star to be of spectral type K0III with a rotational velocity of $v\sin i$=65±9 km s^{-1}, contributing $\sim25\%$ to the observed flux at 6500Å (Shahbaz et al. 1999). 2S 0921–630/V395 Car is one of those rare LMXBs in which the secondary is visible despite the presence of a luminous disc.

There has been no detection of type I X-ray bursts, so the nature of the compact object is unclear. In this letter we present the results of an intensive campaign to measure the dynamical mass of the compact object in 2S 0921–630/V395 Car. We determine the

secondary star's radial velocity curve, investigate the possible effects of X-ray irradiation and obtain firm constraints on the compact object mass.

2. Observations and Data Reduction

Time resolved spectroscopic observations of 2S 0921–630/V395 Car were obtained on the 1.9-m telescope at the South African Astronomical Observatory (SAAO) during 2003 March 30 to April 18. Grating # 5 (1200 lines/mm) was used centered at 4900Å and covering a wavelength range of 4529–5377Åwith a dispersion of $0.49\,\text{Å/pixel}^{-1}$. A slit width of $2.0\,''$gave a spectral resolution of 1.1 Å (=64 km s^{-1} at 5200Å) as measured from the Cu-Arc arc lines. In general the conditions were good, with the seeing varying between $1''$–$3''$. A total of 83 spectra of 2S 0921–630/V395 Car were obtained with an exposure time of 1800 s. Each spectrum was bracketed by an observation of the internal Cu-Ar arc lamp at the position of the star. Template field stars of a variety of spectral types were also observed.

The images were flat-fielded using observations of a tungsten calibration lamp, and a constant bias level was subtracted from all the images. Extraction of the 1-D spectra from the images were performed using optimal extraction (Horne 1986) and calibration of the wavelength scale was achieved using 4th order polynomial fits to the position measured arc-line positions, which gave an rms scatter of ∼0.02 Å.

In addition, 34 spectra were also obtained at the Very Large Telescope (VLT; Paranal, Chile), New Technology Telescope (NTT; La Silla, Chile) the Anglo Australian Telescope (AAT; Siding Springs, Australia) and at the Magellan telescope (Las Campanas, Chile) as part of a long-term project on X-ray binaries. We used the FORS2 Spectrograph attached to the 8.2m Yepun Telescope (VLT) on the nights of 2003 May 18 and June 22-23. A total of 9 spectra with exposure times in the range 300 to 900 s were obtained. The R1400V holographic grating was used in combination with a $0.7\,''$slit resulting in a wavelength coverage of 4514–5815Å and a resolution of 70 km s^{-1}. Instrumental flexure was monitored by cross-correlating the sky spectra and was found to be very small, always within 6 km s^{-1}. The Magellan spectra were obtained on 2003 Dec 12–16 using the Baade telescope at Las Campanas using the IMACS imaging spectrograph in long-camera mode. A total of 11 spectra with an exposure time of 300s were obtained. The 600 grating together with a $0.7\,''$long slit provided spectra covering 3720–6830Å with a dispersion of $0.75\,\text{Å/pixel}^{-1}$. The AAT spectra were obtained using the RGO spectrograph on the nights of 2002 June 6 to 11. A total of 10 spectra with an exposure time of 1800 s were obtained. The R1200B grating centered at 4350Å together with a $1.0\,''$slit provided spectra covering 3500-5250Å with a resolution of 70 km s^{-1}. The total of 4 NTT spectra were obtained with EMMI and grating # 6 on the nights of 2002 June 8 to

10 exposure times of 600 to 900 s. The spectra cover the spectral range 4400–5150Å with a resolution of $75\,\mathrm{km\,s^{-1}}$. The AAT and NTT data reduction details are given in Casares et al. (2003).

3.   The radial velocity curve and spectrum

To increase the signal-to-noise of the spectra prior to cross-correlation, the individual spectra were variance averaged into nighly means or groups of $\sim$3 hrs, depending on the quality of the individual spectra. A total of 31 absorption line radial velocities were measured by cross-correlation (Tonry & Davis 1979) with a template star. Prior to cross-correlation, the spectra were interpolated onto a constant velocity scale ($32\,\mathrm{km\,s^{-1}\,pixel^{-1}}$) and normalized by fitting a spline function to the continuum. The region 5100–5300Å common to all the spectra, primarily containing the MgI (5167.3Å, 5172.7Å and 5183.6Å) absorption blend was used in the analysis. The template star's radial velocity, determined using the position of the FeI 4957.597Å absorption line, was then added to the radial velocities of 2S 0921–630/V395 Car. The resulting radial velocity data (see Figure 1) were then fitted with a circular orbit (sinusoidal function) using the method of least-squares. Using spectral type template stars in the range G6–K4III we obtain K_2 values in the range 92–99 $\mathrm{km\,s^{-1}}$(see Table 1). The secondary star's spectral type has previously been determined from high-resolution spectroscopy to be K0III (Shahbaz et al. 1999), and our work confirms this. Fitting the radial velocities with a K0III template star, we find a minimum reduced χ^2 of 4.3 with the best fit parameters $\gamma = 34.9 \pm 3.3\,\mathrm{km\,s^{-1}}$ $K_2 = 92.89 \pm 3.84\,\mathrm{km\,s^{-1}}$ P_{orb}=9.0035±0.0029 day and T_0=HJD 2453099.51±0.08, where P_{orb} is the orbital period, T_0 is time at phase 0.0 defined as inferior conjunction of the secondary star, γ is the systemic velocity and K_2 is the radial velocity semi-amplitude (1-σ errors are quoted with the error bars rescaled so that the reduced χ^2 of the fit is 1.) Our ephemeris is consistent with that determined by Mason et al. 1987. We also computed a χ^2 periodogram of the data to investigate the significance of other periods. No significant peaks (at >99.99 % level) were present other than the one at 9.0035 day. Finally, to check if the 9.0035 day period is affected by an alias, we computed the window function; no significant peaks were present at 9.0035 day. Fitting the radial velocity data with an eccentric orbit did not yield a better fit; the eccentric fit is only significant at the 38% level.

Using a distance of $\sim$10 kpc Cowley et al. (1982) 2S 0921–630/V395 Car lies 1.6 kpc below the galactic plane and so belongs to the Halo population. Note the systemic velocity is not consistent with the radial velocity due to Galactic differential rotation, $\sim$60 $\mathrm{km\,s^{-1}}$ at a distance of $\sim$10 kpc (Dehnen & Binney 1998). However, what is interesting is that the

magnitude of the systemic velocity of 2S 0921–630/V395 Car seems to be about a factor of ~ 4 lower compared to other neutron star Halo systems (Casares et al. 1998, 2002; Torres et al. 2002).

In Figure 2 we show the variance-weighted Doppler averaged spectrum of V395 Car. The strongest features are the H, He emission lines, which appear single peaked, even at the resolution of these data. Weak absorption features of Mg I 5175Å and the Ca/Fe blend at 5269Å allow us to determine the fraction of light from the secondary star, by optimally subtracting a scaled K0III template spectrum from V395 Car (Marsh et al. 1994). As the rotational broadening of the donor (65 ± 9 km s^{-1}; Shahbaz et al. 1999) is similar to our spectral resolution (64 km s^{-1}), we do not broaden the template before subtraction. We find that the secondary star contributes $\sim 10\%$ to the observed flux at 5200Å (see Table 1).

4. Irradiation of the secondary star - the mass of the compact object

The observed X-rays are reflected into our line of sight by scattering. Although the observed X-ray luminosity is low $L_X = 2 \times 10^{35}$ erg s^{-1} (Kallman et al. 2003), it is still interesting to explore the possible effects that X-rays may have on the secondary star's atmosphere and hence radial velocity. We investigate these effects using the X-ray binary model described by Phillips et al. (1999); Shahbaz et al. (2000, 2003). We first phase-folded the radial velocities using the orbital ephemeris derived in section 3 and binned into 31 orbital phase bins. We then fit the resulting radial velocity curve with the X-ray binary model. We considered two extreme cases for the X-ray irradiation: case (a) where the X-rays produced near the compact object irradiate the whole inner face of the secondary star and case (b) where the X-ray's do not affect the secondary star. Note that invoking a flared accretion disc will have intermediate solutions. The variable model parameters are the compact object mass M_1, secondary star mass M_2, X-ray luminosity L_X and the inclination i. To determine which elements on the star contribute to the absorption line radial velocity we use the factor f_X, which is the fraction of the external radiation flux that exceeds the unperturbed flux. For a given i and combination of M_1 and M_2 we fit the data and use the constraints imposed by the measured value for $v \sin i$ (64 ± 9 km s^{-1}; Shahbaz et al. 1999) to produce plots in the M_1–M_2 plane (Figure 3)

Given the evidence for optical and X-ray partial eclipse, i must lie in the range 70°–90°. Therefore we consider cases (a) and (b) for i=70° and more importantly i=90°, because it gives a firm lower limit to the compact object's mass. For case (a) we fix $L_X = 2 \times 10^{35}$ erg s^{-1} and find that the best fit ($\chi^2 = 122$) is obtained when all the elements on the inner face contribute to the radial velocity, i.e. $f_X > 60\%$, i.e. X-ray heating is not preferred. Note,

however, that the radial velocity curve will not be sinusoidal because there will still be some irradiated elements that contribute to the radial velocity. Even if we increase to $L_X = 10^{39} \, \mathrm{erg \, s^{-1}}$ as could be the case for an LMXB, the fits are significantly worse ($\chi^2 = 190$) and the best fit still occurs when all the inner face contributes to the radial velocity. For case (b) we set $L_X = 0$, implying no X-ray heating and find that it gives a fit with similar quality ($\chi^2 = 119$). We conclude that the best fit to the radial velocity curve is the case where the X-rays do not have an observable effect given the quality of the data. For our range in i our fits for case (a) and (b) give $2.0 < M_1 < 4.3 \, \mathrm{M_\odot}$ (1-σ), which means we can rule out a canonical $1.4 \, \mathrm{M_\odot}$ neutron star at the 99% level. Our solutions for the compact object mass suggests either a massive neutron star or a low-mass black hole, since the maximum mass allowed for a neutron star is $2.9 \, \mathrm{M_\odot}$ (Kalogera & Baym 1996).

Since the donor star fills its Roche lobe and is synchronized with the binary motion, we use the secondary star's $v \sin i$ and K_2 to determine the binary mass ratio $q = (M_2/M_1) = 0.89 \pm 0.18$ (Horne et al. 1986). Given the measured masses and orbital period, we use Kepler's Third Law to determine the semi-major axis $56.1 < a < 72.4 \, \mathrm{R_\odot}$. Eggleton's (1983) expression for the effective radius of the Roche-lobe then determines the radius of the secondary $10.4 < R_2 < 13.4 \, \mathrm{R_\odot}$, and the temperature inferred from the spectral type (Gray 1992) and Stefan-Boltzmann's law determines the luminosity $52.5 < L_2 < 87.1 \, \mathrm{L_\odot}$ (1-σ ranges are quoted).

5. Discussion

5.1. The evolutionary status of the system

The position of the secondary star of 2S 0921–630/V395 Car in an HR diagram corresponds to a normal star that has crossed the Hertzsprung gap and now lies on the Hayashi line. The evolution of the binary is dominated by the evolution of the evolved secondary star. Since such a star no longer burns hydrogen in its core, the mass transfer is early massive Case B. For a binary with a secondary star near the onset of such mass transfer, one requires $q < 1$ throughout its history (King & Ritter 1999). The case for a $1.4 \, \mathrm{M_\odot}$ neutron star can be ruled out since it requires $M_2 < 1.4 \, \mathrm{M_\odot}$, which is inconsistent with our results; the position of a secondary on the HR diagram undergoing early massive Case B mass transfer is close to that of a single star of the same mass (Kolb 1998). For a $3 \, \mathrm{M_\odot}$ compact object, $M_2 < 3.0 \, \mathrm{M_\odot}$, which is consistent with our observations.

It is interesting to note that the mass ratio we derive lies on the limit of stable/unstabe mass transfer $q = 5/6$ (King & Ritter 1999). It is possible that 2S 0921–630/V395 Car is

undergoing unstable mass transfer similar to the supersoft sources and other X-ray binaries (Kahabka & van den Heuvel 1997).

5.2. The formation of the compact object

The distribution of measured neutron stars masses provides fundamental constraints on the equation of state of nuclear matter and the observational identification of a black hole which is based on the maximum gravitational mass allowed for a neutron star; 2.9 $M_\odot$ (Kalogera & Baym 1996). Studies of radio pulsars show that neutron star masses are clustered in a narrow range. However, there is some evidence that neutron stars with a mass in excess of 1.4 $M_\odot$ do exist. LMXBs are expected to contain massive ($\sim$2 $M_\odot$) neutron stars, resulting from the accretion of a considerable amount of material over extended (10^8 yrs) periods of time (Zhang et al. 1985). However, while a neutron star mass of 1.78$\pm$0.23 $M_\odot$ for the LMXB Cyg X-2 is reported (Orosz & Kuulkers 1999), Titarchuk & Shaposhnikov (2002) have recently proposed a mass of 1.44$\pm$0.06 $M_\odot$ based on the spectral and temporal properties of the type I X-ray bursts. The analysis of optical data for the X-ray pulsar Vela X-1 suggests that the pulsar has a mass of $1.87^{+0.23}_{-0.17}$ $M_\odot$ (Barziv et al. 2002). Probably the strongest case for a massive neutron star or low-mass black hole is in the eclipsing HMXB 4U 1700–37 which contains a 2.44$\pm$0.27 $M_\odot$ compact object (Clark et al. 2002). Such masses already test soft nuclear equations of state (Miller et al. 1998a). We obtain a mass of 2.0–4.3 $M_\odot$ for the compact object in 2S 0921–630/V395 Car, which lies between the range of masses observed for neutron stars and black holes. Models for nuclear equations of state which include the effects of three nucleon interactions and realistic models of nuclear forces limits the maximum mass of neutron stars to be below 2.5 $M_\odot$(Akmal et al. 1998). However, it should be noted that unconventional forms of matter such as Q-stars do allow the existence of extremely massive neutron stars (Miller et al. 1998b) Although our results do not allow us to distinguish between a massive neutron star or a low mass black hole, the existence of a >2.5 $M_\odot$neutron star would place strong constraints on high density nuclear matter.

Theoretical predictions by Fryer & Kalogera (2001) suggest that the death of a 60 $M_\odot$ star in a close binary system can produce anything from a low-mass 1.2 $M_\odot$ neutron star to a 10 $M_\odot$ black hole, depending on the wind mass-loss rate during the Wolf-Rayet phase. As suggested by Brown et al. (1996) the formation of a low-mass black hole with a high space velocity is possible via a two stage process involving the formation of a neutron star. However, if there is symmetric mass ejection in the supernova, then a kick at the formation of a black hole is not required to explain the varied range in the observed space velocities of the black hole LMXBs (Nelemans et al. 1999).

The unusual mass for the compact object in 2S 0921–630/V395 Car and the fact that the nature of the compact object is not clear, conjours up many formation scenarios. If it is a neutron star, then its present mass can be explained by either the accumulation of matter (1–2 $M_\odot$) by a canonical 1.4 $M_\odot$ neutron star, accreted at a high mass accretion rate over a long period of time, or the direct collapse of a massive star forming a massive neutron star. If the compact object in 2S 0921–630/V395 Car is a black hole then its low mass can be explained by the accretion induced collapse of a massive 2.9 $M_\odot$ neutron star or the formation of a low-mass black hole (Brown et al. 1996). Given the fact that we do not observe a peculiar systemic velocity comparable to other neutron-star LMXBs, this suggests that we can rule out canonical neutron star formation scenarios where a kick is produced during a type II supernova. The most likely scenario for the formation of the compact object is the direct formation of a massive neutron star or a low-mass black hole.

REFERENCES

Akmal, A., Pandharipande, V. R., & Ravenhall, D. G. 1998, Phys. Rev. C, 58, 1804

Barziv O., Kaper L., van Kerkwijk M. H., Telting J. H., van Paradijs J., 2001, A&A, 377, 925

Branduardi-Raymont, G., Corbet, R. H. D., Mason, K. O., Parmar, A. N., Murdin, P. G., & White, N. E. 1983, MNRAS, 205, 403

Brown G. E., Weingartner J. C., Wijers Ralph A. M. J., 1996, ApJ, 463, 297.

Casares, J., Charles, P. A., & Kuulkers, E. 1998, ApJ, 493, L39

Casares, J., Dubus, G., Shahbaz, T., Zurita, C., & Charles, P. A. 2002, MNRAS, 329, 29

Casares, J., Steeghs, D., Hynes, R. I., Charles, P. A., & O'Brien, K. 2003, ApJ, 590, 1041

Charles P. A., Coe M., in Compact Stellar X–ray Sources, ed. W. H. G. Lewin & M. van der Klis, Cambridge University Press, astro-ph/0308020

Chevalier, C. & Ilovaisky, S. A. 1982, A&A, 112, 68

Chevalier, C. & Ilovaisky, S. A. 1981, A&A, 94, L3

Clark, J. S., Goodwin, S. P., Crowther, P. A., Kaper, L., Fairbairn, M., Langer, N., & Brocksopp, C. 2002, A&A, 392, 909

Cowley, A. P., Crampton, D., & Hutchings, J. B. 1982, ApJ, 256, 605

Dehnen, W. & Binney, J. 1998, MNRAS, 294, 429

Fryer, C. L. & Kalogera, V. 2001, ApJ, 554, 548

Gray, D. F. 1992, Cambridge Astrophysics Series, Cambridge: Cambridge University Press, 1992, 2nd ed.

Horne, K. 1986, PASP, 98, 609

Horne, K., Wade, R. A., & Szkody, P. 1986, MNRAS, 219, 791

Kahabka, P. & van den Heuvel, E. P. J. 1997, ARA&A, 35, 69

Kallman, T. R., Angelini, L., Boroson, B., & Cottam, J. 2003, ApJ, 583, 861

Kalogera, V. & Baym, G. 1996, ApJ, 470, L61

King, A. R. & Ritter, H. 1999, MNRAS, 309, 253

Li, F. K., Clark, G. W., Jernigan, J. G., Laustsen, S., Zuiderwijk, E. J., & van Paradijs, J. A. 1978, Nature, 276, 799

Kolb, U. 1998, MNRAS, 297, 419

Marsh, T. R., Robinson, E. L., & Wood, J. H. 1994, MNRAS, 266, 137

Mason, K. O., Branduardi-Raymont, G., Codova, F. A., & Corbet, R. H. D. 1987, MNRAS, 226, 423

Miller, M. C., Lamb, F. K., & Psaltis, D. 1998a, ApJ, 508, 791

Miller, J. C., Shahbaz, T., & Nolan, L. A. 1998b, MNRAS, 294, L25

Nelemans, G., Tauris, T. M., & van den Heuvel, E. P. J. 1999, A&A, 352, L87

Orosz J. A., Kuulkers E., 1999, MNRAS, 305, 132.

Phillips, S. N., Shahbaz, T., & Podsiadlowski, P. 1999, MNRAS, 304, 839

Shahbaz, T., Kuulkers, E., Charles, P. A., van der Hooft, F., Casares, J., & van Paradijs, J. 1999, A&A, 344, 101

Shahbaz, T., Groot, P., Phillips, S. N., Casares, J., Charles, P. A., & van Paradijs, J. 2000, MNRAS, 314, 747

Shahbaz, T., Zurita, C., Casares, J., Dubus, G., Charles, P. A., Wagner, R. M., & Ryan, E. 2003, ApJ, 585, 443

Thorstensen, J. R. & Charles, P. A. 1979, BAAS, 11, 721

Titarchuk, L. & Shaposhnikov, N. 2002, ApJ, 570, L25

Tonry, J. & Davis, M. 1979, AJ, 84, 1511

Torres, M. A. P., Casares, J., Martínez-Pais, I. G., & Charles, P. A. 2002, MNRAS, 334, 233

van Kerkwijk, M. H. 2001, in Black Holes in Binaries and Galactic Nuclei, ed. L. Kaper, E. P. J. van den Heuvel, & P. A. Woudt (Berlin: Springer), 39

White, N. E. & Mason, K. O. 1985, Space Science Reviews, 40, 167

White, N. E., Nagase, F., Paramar, A. N., 1995, X-ray Binaries, eds. W.H.G. Lewin, J. van Paradijs, and E.P.J. van den Heuvel (Cambridge: Cambridge Univ. Press), p. 1

Zhang W., Strohmayer T. E., Swank J. H., 1997, ApJ, 482, L167.

Table 1: Fits to the radial velocity curve of $2S\,0921$–630/V395 Car (1-σ errors are given).

| Template	SpT	γ	P_{orb}	T_0 *	K_2	χ^2_ν	f
		$(\mathrm{km\,s^{-1}})$	day)		$(\mathrm{km\,s^{-1}})$		%
HD122571	G6III	33.3 (3.8)	9.0019(36)	9.54(10)	95.1(4.4)	5.8	6.7
HD63513	G7III	34.2 (3.6)	9.0017(32)	9.53(9)	94.2(3.7)	5.3	7.8
HD40359	G8III	36.9 (3.1)	9.0040(30)	9.51(9)	92.2(3.7)	4.5	8.6
HD71863	G9III	35.1 (3.3)	9.0027(29)	9.51(8)	93.9(3.8)	4.3	9.6
HD82565	K0III	34.9 (3.3)	9.0035(29)	9.51(8)	92.9(3.8)	4.3	9.9
HD39523	K1III	37.6 (3.2)	9.0036(28)	9.53(7)	94.3(3.7)	4.6	9.0
HD61248	K3III	41.0 (3.5)	9.0062(32)	9.58(7)	96.5(4.1)	6.1	7.9
HD40522	K4III	42.0 (3.7)	9.0057(34)	9.59(7)	98.6(4.3)	6.0	8.2

∗HJD 2453099+
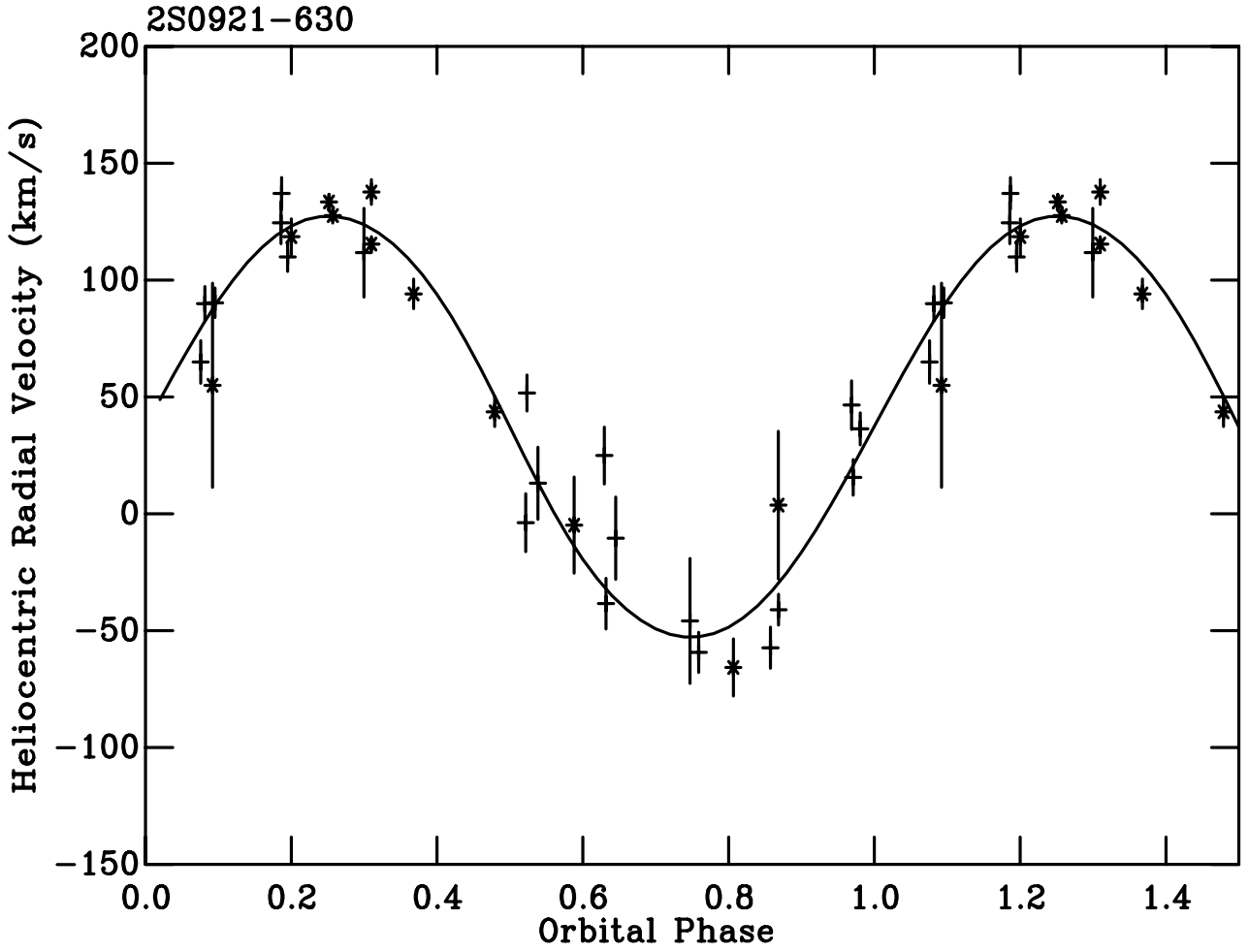
Fig. 1.— The heliocentric radial velocity curve of the secondary star. The crosses show the SAAO data and the stars the VLT, NTT, AAT and Magellan data. The solid line shows a sinusoidal fit to the data. The data have been folded on the orbital ephemeris and 1.5 orbital cycles are shown for clarity.
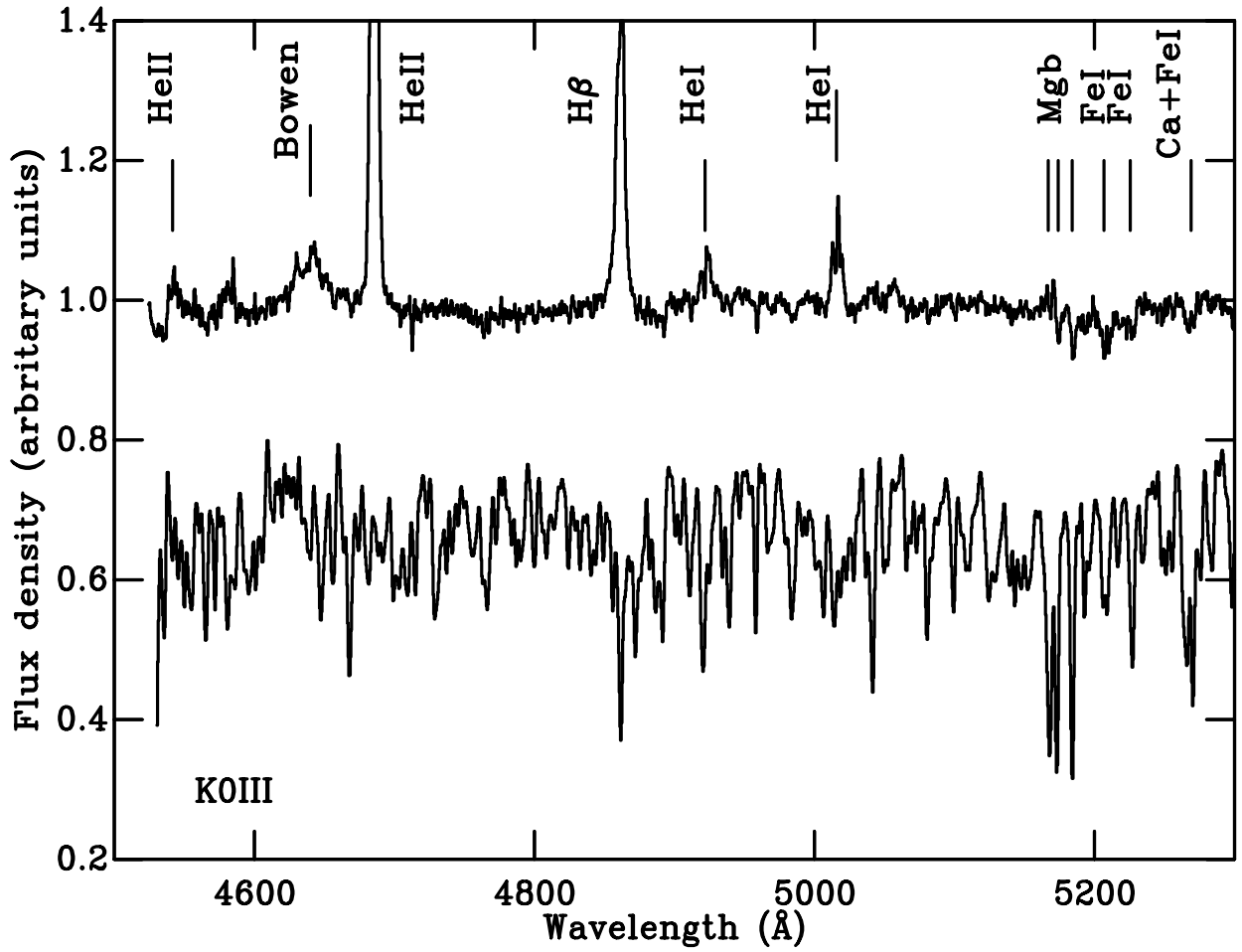
Fig. 2.— Top: the variance-weighted Doppler shifted average spectrum of 2S 0921–630/V395 Car in the rest frame of the secondary star. The most noticeable features are the H and He emission lines arising from the accretion disc. Bottom: the K0III spectral type template star HD82565. The spectra have been normalized and shifted vertically for clarity.
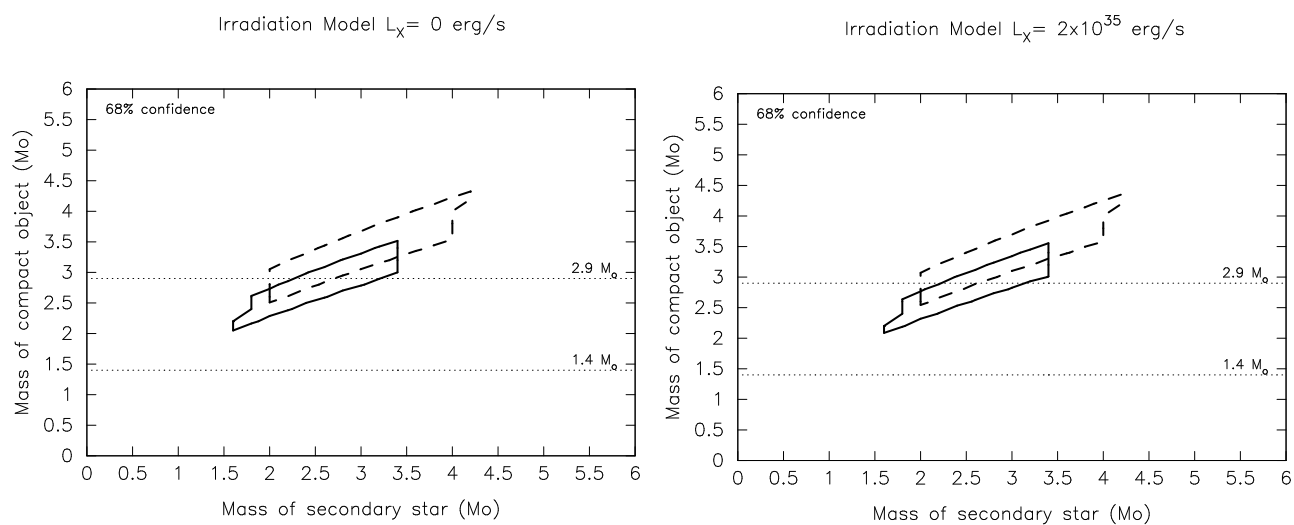
Fig. 3.— The effects of X-ray heating on the secondary star's radial velocity curve and hence the allowed binary component masses. The left and right plots show the case without and with X-ray heating respectively. The solid and dashed contours show the 68% confidence level obtained by fitting the radial velocity curve with the X-ray binary model using $i=90°$ and 70° respectively (see section 4) The dotted horizontal lines mark 1.4 $M_\odot$ and 2.9 $M_\odot$, and represent the canonical and maximum neutron star mass respectively.